

Helices versus Zigzag Chains: One-Dimensional Coordination Polymers of Ag^I and Bis(4-pyridyl)amine

David B. Cordes,[†] Lyall R. Hanton,*[†] and Mark D. Spicer[‡]

Department of Chemistry, University of Otago, PO Box 56, Dunedin, New Zealand, and Department of Pure and Applied Chemistry, University of Strathclyde, 295 Cathedral Street, Glasgow G1 1XL, Scotland

Received March 23, 2006

Five one-dimensional coordination polymers were prepared by the reaction of a bent bridging ligand, bis(4-pyridyl)amine (**bpa**), with an extensive series of AgX salts (X = CF₃SO₃, PF₆, ClO₄, NO₃). The 1D polymer networks formed with AgCF₃SO₃ (**1**), AgPF₆ (**2**·MeCN), and AgClO₄ (**3**·2MeCN) all incorporated MeCN and were found to adopt a zigzag arrangement. The networks formed with AgClO₄ (**4**) and AgNO₃ (**5**) did not contain any solvent and adopted a single-stranded helical arrangement. Two-dimensional H-bonding networks were formed for **1** and **3**·2MeCN, with network topologies 4.8² and (4, 4), respectively, whereas three-dimensional H-bonded networks of helices were formed for **4**, showing an (8, 3)-a network topology, and **5**, showing the topology of the α-polonium net. The three-dimensional networks both exhibited 4-fold interpenetration. The NO₃⁻ anion in **5** appeared to be acting as a template for the 3D structure.

Introduction

The programmed self-assembly of coordination networks has attracted intense interest not least because of the intricate structural topologies that can be created.¹ Seemingly simple one-dimensional polymers can be found to show highly unusual topologies when additional directional interactions are considered.² Linear bridging ligands such as pyrazine or 4,4'-bipyridine were among the first ligands used in the specific formation of coordination polymers because they were simple, readily available, and looked to allow for more predictable formation of network structures.³ In contrast, the use of bridging ligands, which are equally simple but incorporate a bend in their structure between donor atoms, allows for major differences in the resulting architectures,

because adjustments in the framework must occur to accommodate the bend of the molecule.⁴ One such simple bent ligand is bis(4-pyridyl)amine (**bpa**) (Figure 1). In addition to its bend, this ligand has two significant features that are able to assist in the formation of supramolecular arrays. First, when **bpa** is conformationally locked in the solid state, it contains a chiral axis and can behave as a two-bladed chiral molecular propeller.⁵ The two enantiomers resulting from the chiral axis differ only in the rotation of the pyridine rings. When not in the solid state, the interconversion of the two forms depends on the barrier to rotation about the amine N–C bond. The two rotational energy maxima (rotation of both pyridine rings through or orthogonal to the molecular plane) have been calculated to be approximately 45 and 20 kJ mol⁻¹, respectively.⁶ These values are sufficiently low that **bpa** would be expected to be achiral in solution.

Second, the central amine of **bpa** is a hydrogen-bonding synthon. Potential hydrogen-bond acceptors are common in supramolecular systems, with other ligands, anions, or solvent molecules all available. The two possible outcomes of the formation of hydrogen bonds in coordination polymers are either an increase in dimensionality or the modification of

* To whom correspondence should be addressed. E-mail: lhanton@alkali.otago.ac.nz.

[†] University of Otago.

[‡] University of Strathclyde.

- (1) (a) Champness, N. R. *Dalton Trans.* **2006**, 877–880. (b) Andruh, M. *Pure Appl. Chem.* **2005**, *77*, 1685–1706. (c) Batten, S. R. *J. Solid State Chem.* **2005**, *178*, 2475–2479. (d) Hosseini, M. W. *Acc. Chem. Res.* **2005**, *38*, 313–323.
- (2) (a) Ye, B.-H.; Tong, M.-L.; Chen, X.-M. *Coord. Chem. Rev.* **2005**, *249*, 545–565. (b) Beatty, A. M. *CrystEngComm* **2001**, *3*, 243–255.
- (3) (a) Zaworotko, M. J. *Chem. Commun.* **2001**, 1–9. (b) Hagrman, P. J.; Hagrman, D.; Zubieta, J. *Angew. Chem., Int. Ed.* **1999**, *38*, 2638–2684. (c) Blake, A. J.; Champness, N. R.; Hubberstey, P.; Li, W.-S.; Withersby, M. A.; Schröder, M. *Coord. Chem. Rev.* **1999**, *183*, 117–138.

(4) Jung, O.-S.; Kim, Y. J.; Lee, Y.-A.; Park, J. K.; Chae, H. K. *J. Am. Chem. Soc.* **2000**, *122*, 9921–9925.

(5) Eliel, E. L.; Wilen, S. H.; Mander, L. N. *Stereochemistry of Organic Compounds*; Wiley-Interscience: New York, 1994; pp 1156–1160.

(6) Benedix, R.; Hennig, H. Z. *Chem.* **1984**, *24*, 303–304.

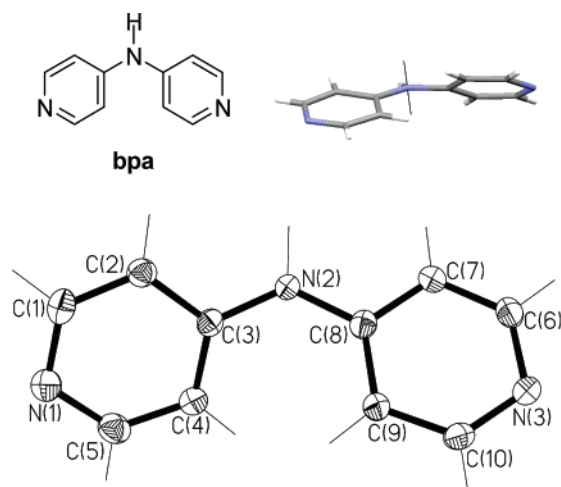


Figure 1. (top left) Ligand **bpa**. (top right) View of **bpa** as a two-bladed chiral propeller showing the chiral axis of one enantiomer. (bottom) View down the crystallographic a -axis of **bpa**. Thermal ellipsoids have been drawn at the 50% probability level.

the polymer without changing its dimensionality. With the correct positioning of donor and acceptor, hydrogen-bond formation may also lead to the formation of interpenetrated nets.⁷ In addition, appropriate positioning of hydrogen-bonding synthons can lead to the formation of templated supramolecular arrays, particularly using often symmetric species such as anions. However, the identification of anion templating in coordination polymers is difficult because of the tendency for anions to coordinate to metal centers, making their role an ambiguous one.⁸ When anions are not coordinated to metal centers but found to be interacting solely with the coordination-polymer framework, they may be templating the formation of the final network structure through a combination of weak supramolecular interactions.

When the one-dimensional coordination-polymeric products formed using such bent ligands are considered, it can be seen that they will usually give rise to either zigzag or helical structures as a result of their shape. Helices provide one of the best examples of the use of chirality in coordination-polymer chemistry. However, the factors underlying the predictable formation of coordination helices are still not well understood, despite the interest in this area.⁹ Chiral ligands can be employed to synthesize helices as either enantiopure or racemic forms. If enantiopure ligands are used, the stereoselective synthesis of helices often results, whereas racemic mixtures of ligands can give crystals that are either racemic or conglomerates of enantiopure crystals. If the coordination arrangements about the metal ions are correct, a zigzag polymer could be changed to a helical one by

changing the auxiliary ligands or the interacting solvent molecules to promote coiling of the structure rather than zigzagging.¹⁰

A technique for the synthesis of coordination polymers that has seen an increase in use recently is hydrothermal synthesis,¹¹ as it reduces or eliminates the problem of differing solubility of precursors. As a result, hydrothermal synthesis can be used for a wide variety of systems. Because of the conditions that occur during hydrothermal synthesis, the crystallization of metastable kinetic products rather than thermodynamic products can also occur as a result of self-assembly reactions.¹² This potential for kinetic control of product formation can provide unusual structural contrasts to materials crystallized under thermodynamic control.

The ligand **bpa** has been used previously in the synthesis of network structures; however, the complexes produced were metal-oxide systems augmented by the addition of **bpa**, and all were synthesized hydrothermally.¹³ Additionally, we have previously synthesized three copper complexes, two two-dimensional, $\{[(\text{Cu}_2\text{I}_2)(\text{bpa})_2]_\infty\}$ and $\{[\text{Cu}(\text{bpa})_2\text{Cl}_2] \cdot 3\text{DMF} \cdot 1\frac{1}{2}\text{H}_2\text{O}\}_\infty$, and one discrete, $[\text{Cu}(\text{bpaH})_2(\text{SO}_4)_2 \cdot (\text{H}_2\text{O})_2] \cdot 4\text{H}_2\text{O}$.¹⁴ These complexes are the first structurally characterized complexes of **bpa** that were not prepared hydrothermally. All the previously prepared **bpa** complexes have shown extensive intermolecular interactions, with a number of structures being extended to two or three dimensions by the formation of hydrogen bonds. Herein, we report the investigation of the effects of differing anions on Ag^{I} coordination polymers of **bpa**. The resulting polymers may be divided into either zigzag or helical one-dimensional polymers. Despite these gross similarities, the resulting weakly interacting two- or three-dimensional supramolecular architectures show great diversity, with two-dimensional networks formed by both hydrogen-bonding and π - π stacking and three-dimensional architectures showing 4-fold interpenetration and, in one case, evidence of anion templating.

Experimental Section

General. The ligand **bpa** was prepared according to the literature method.^{13g} Infrared spectra were measured on a Perkin–Elmer Win-

- (7) For example, see: (a) Stephenson, M. D.; Hardie, M. J. *Cryst. Growth Des.* **2006**, *6*, 423–432. (b) Bradshaw, D.; Rosseinsky, M. J. *Solid State Sci.* **2005**, *7*, 1522–1532. (c) Vreshch, V. D.; Lysenko, A. B.; Chernega, A. N.; Sieler, J.; Domasevitch, K. V. *Polyhedron* **2005**, *24*, 917–926. (d) Qin, C.; Wang, X.; Carlucci, L.; Tong, M.; Wang, E.; Hu, C.; Xu, L. *Chem. Commun.* **2004**, 1876–1877. (e) Matthews, C. J.; Elsegood, M. R. J.; Bernardinelli, G.; Clegg, W.; Williams, A. F. *Dalton Trans.* **2004**, 492–497. (f) Batten, S. R. *CrystEngComm* **2001**, *3*, 67–73 and references therein.
- (8) Vilar, R. *Angew. Chem., Int. Ed.* **2003**, *42*, 1460–1477.
- (9) (a) Han, L.; Hong, M. *Inorg. Chem. Commun.* **2005**, *8*, 406–419. (b) Kesanli, B.; Lin, W. *Coord. Chem. Rev.* **2003**, *246*, 305–326.

- (10) (a) Chen, X.-D.; Mak, T. C. W. *J. Mol. Struct.* **2005**, *743*, 1–6. (b) Ezuhara, T.; Endo, K.; Aoyama, Y. *J. Am. Chem. Soc.* **1999**, *121*, 3279–3283.
- (11) For example, see: (a) Qin, C.; Wang, X.-L.; Li, Y.-G.; Wang, E.-B.; Su, Z.-M.; Xu, L.; Clérac, R. *Dalton Trans.* **2005**, 2609–2614. (b) Kim, Y. J.; Park, Y. J.; Jung, D.-Y. *Dalton Trans.* **2005**, 2603–2609. (c) Domasevitch, K. V.; Boldog, I.; Rusanov, E. B.; Hunger, J.; Blaurock, S.; Schröder, M.; Sieler, J. Z. *Anorg. Allg. Chem.* **2005**, *631*, 1095–1100. (d) Kim, D. S.; Forster, P. M.; Le Toquin, R.; Cheetham, A. K. *Chem. Commun.* **2004**, 2148–2149.
- (12) Gopalakrishnan, J. *Chem. Mater.* **1995**, *7*, 1265–1275.
- (13) (a) *Inorg. Chim. Acta* **2002**, *340*, 211–214. (b) LaDuca, R. L., Jr.; Rarig, R. S., Jr.; Zubieta, J. *Inorg. Chem.* **2001**, *40*, 607–612. (c) LaDuca, R. L., Jr.; Finn, R.; Zubieta, J. *Chem. Commun.* **1999**, 1669–1670. (d) LaDuca, R. L., Jr.; Rarig, R. S., Jr.; Zapf, P. J.; Zubieta, J. *Inorg. Chim. Acta* **1999**, *292*, 131–136. (e) Laskoski, M. C.; LaDuca, R. L., Jr.; Rarig, R. S., Jr.; Zubieta, J. *J. Chem. Soc., Dalton Trans.* **1999**, 3467–3472. (f) Hargman, D.; Warren, C. J.; Haushalter, R. C.; Seip, C.; O'Connor, C. J.; Rarig, R. S., Jr.; Johnson, K. M., III; LaDuca, R. L., Jr.; Zubieta, J. *Chem. Mater.* **1998**, *10*, 3294–3297. (g) Zapf, P. J.; LaDuca, R. L., Jr.; Rarig, R. S., Jr.; Johnson, K. M., III; Zubieta, J. *Inorg. Chem.* **1998**, *37*, 3411–3414.
- (14) Cordes, D. B.; Hanton, L. R.; Spicer, M. D. *J. Mol. Struct.* **2006**, in press.

Table 1. Crystallographic Data for Complexes

	bpa	1	2·MeCN	3·2MeCN	4	5
formula	C ₁₀ H ₉ N ₃	C ₁₃ H ₁₂ AgF ₃ N ₄ O ₃ S	C ₁₂ H ₁₂ AgF ₆ N ₄ P	C ₂₈ H ₃₀ Ag ₂ Cl ₂ N ₁₀ O ₈	C ₁₀ H ₉ AgClN ₃ O ₄	C ₁₀ H ₉ AgN ₄ O ₃
mol wt	171.2	469.20	465.10	921.26	378.52	341.08
cryst syst	orthorhombic	monoclinic	monoclinic	monoclinic	hexagonal	trigonal
space group	<i>P</i> 2 ₁ <i>ca</i> (No. 29)	<i>P</i> 2 ₁ / <i>c</i> (No. 14)	<i>P</i> 2 ₁ / <i>c</i> (No. 13)	<i>P</i> 2 ₁ / <i>c</i> (No. 14)	<i>P</i> 6 ₅ 22 (No. 179)	<i>R</i> 32 (No. 155)
<i>a</i> (Å)	7.3221(5)	10.3980(9)	7.9029(7)	7.324(2)	8.0101(3)	9.459(4)
<i>b</i> (Å)	9.7525(7)	23.6320(19)	9.8007(9)	23.444(8)	8.0101(3)	9.459(4)
<i>c</i> (Å)	11.8921(10)	6.9900(6)	20.5060(19)	19.550(6)	33.3449(10)	34.558(14)
β (deg)		107.067(1)	99.297(2)	91.168(6)		
<i>U</i> (Å ³)	849.20(11)	1642.0(2)	1567.4(2)	3356.3(19)	1852.68(10)	2677.7(19)
<i>Z</i>	4	4	4	4	6	9
<i>T</i> (K)	123(2)	163(2)	98(2)	111(2)	173(2)	123(2)
μ (mm ⁻¹)	0.084	1.408	1.455	1.391	1.862	1.7
no. of reflns collected	3248	10879	13387	25136	8938	2105
no. of unique reflns (<i>R</i> _{int})	1046 (0.0530)	3333 (0.0164)	3214 (0.0289)	6744 (0.0781)	1764 (0.0555)	867 (0.0206)
<i>R</i> 1 indices [<i>I</i> > 2 σ (<i>I</i>)]	0.0436	0.0276	0.0268	0.1060	0.0310	0.0492
w <i>R</i> 2 (all data)	0.0849	0.0735	0.0630	0.2883	0.0676	0.1291

IR Spectrum BX FT-IR system (samples in KBr disks). Elemental analyses were performed by the Campbell Microanalytical laboratory at the University of Otago. Samples were predried under a vacuum to remove volatile solvent residues.

Caution: Although no problems were encountered in this work, transition-metal perchlorates are potentially explosive. They should be prepared in small amounts and handled with care.

Preparation of Ag^I Coordination Polymers. {[Ag(**bpa**)(MeCN)]-(CF₃SO₃)₃]_∞ (**1**). AgCF₃SO₃ (75 mg, 0.29 mmol) dissolved in degassed MeCN (20 mL) was added via cannula to **bpa** (50 mg, 0.29 mmol) dissolved in degassed MeCN–H₂O (20 mL, 3:1, v/v) and stirred overnight. The resulting solution was reduced in volume to 5 mL, and diethyl ether was added. The white solid that immediately precipitated was filtered and dried in vacuo. Yield: 80 mg (64%). Colorless X-ray quality crystals were grown from the slow diffusion of an *i*PrOH solution of **bpa** layered with MeCN and a H₂O solution of AgCF₃SO₃. Anal. Calcd for C₁₁H₉N₃O₃F₃SAg: C, 30.85; H, 2.12; N, 9.82; F, 13.31; S, 7.49. Found: C, 30.49; H, 1.95; N, 9.69; F, 7.25; S, 7.49. Selected IR (KBr, cm⁻¹): 3415m (**bpa**), 1252s br (CF₃SO₃⁻), 1168m br (CF₃SO₃⁻), 1030s (CF₃SO₃⁻), 532m (**bpa**).

{[Ag(**bpa**)](PF₆)₃]_∞ (**2**). AgPF₆ (74 mg, 0.29 mmol) dissolved in degassed MeCN–H₂O (20 mL, 3:1, v/v) was added via cannula to **bpa** (50 mg, 0.29 mmol) dissolved in degassed MeCN–H₂O (20 mL, 3:1, v/v) and stirred for 3 days. The resulting solution was reduced in volume to 5 mL, and diethyl ether was added. The white solid that immediately precipitated was filtered and dried in vacuo. Yield: 88 mg (71%). Colorless X-ray quality crystals of **2·MeCN** were grown from the slow diffusion of an *i*PrOH solution of **bpa** layered with MeCN and a H₂O solution of AgPF₆. Anal. Calcd for C₁₀H₉N₃F₆PAg: C, 28.32; H, 2.14; N, 9.91. Found: C, 28.13; H, 2.33; N, 9.84. Selected IR (KBr, cm⁻¹): 3403m (**bpa**), 842s br (PF₆⁻), 530m (**bpa**).

{[Ag(**bpa**)](ClO₄)₃]_∞ (**3**). AgClO₄ (61 mg, 0.29 mmol) dissolved in degassed MeCN–H₂O (20 mL, 3:1, v/v) was added via cannula to **bpa** (50 mg, 0.29 mmol) dissolved in degassed MeCN–H₂O (20 mL, 3:1, v/v) and stirred overnight. The white solid that precipitated was filtered and dried in vacuo. Yield: 74 mg (67%). Colorless X-ray quality crystals of **3·2MeCN** were grown from the slow diffusion of a 2,2,2-trifluoroethanol solution of **bpa** layered with MeNO₂ and an MeCN solution of AgClO₄. Anal. Calcd for C₁₀H₉N₃O₄ClAg: C, 31.72; H, 2.40; N, 11.10. Found: C, 31.62; H, 2.69; N, 11.33. Selected IR (KBr, cm⁻¹): 3416m (**bpa**), 1084s (ClO₄⁻), 528m (**bpa**).

Hydrothermal Synthesis of {[Ag(bpa**)](ClO₄)₃]_∞ (**4**).** AgClO₄ (12 mg, 58 μmol) and **bpa** (10 mg, 58 μmol) were combined in a

5 mL Pyrex tube with H₂O (2 mL). The tube was taken through 2 cycles of freeze–pump–thaw and then sealed. It was placed in a thick-walled steel blast tube, heated to 120 °C for 64 h, and then allowed to cool slowly to room temperature. Colorless X-ray quality crystals were isolated from a white fluffy gel. Yield: 7.7 mg (35%).

{[Ag(**bpa**)](NO₃)₃]_∞ (**5**). AgNO₃ (50 mg, 0.29 mmol) dissolved in degassed MeCN (20 mL) was added via cannula to **bpa** (50 mg, 0.29 mmol) dissolved in degassed MeCN–H₂O (20 mL, 3:1, v/v) and stirred overnight. The white solid that precipitated was filtered and dried in vacuo. Yield: 78 mg (78%). Colorless X-ray quality crystals were grown from the slow diffusion of a MeCN/H₂O solution of **bpa** layered with benzene and a MeCN solution of AgNO₃. Anal. Calcd for C₁₀H₉N₄O₃Ag: C, 35.21; H, 2.66; N, 16.43. Found: C, 35.50; H, 2.69; N, 16.32. Selected IR (KBr, cm⁻¹): 3418m (**bpa**), 1351s (NO₃⁻), 531m (**bpa**).

Hydrothermal Synthesis of {[Ag(bpa**)](NO₃)₃]_∞ (**5**).** AgNO₃ (9.9 mg, 58 μmol) and **bpa** (10 mg, 58 μmol) were combined in a 5 mL Pyrex tube with H₂O (2 mL). The tube was taken through 2 cycles of freeze–pump–thaw and then sealed. It was placed in a thick-walled steel blast tube, heated to 120 °C for 2 days, and then allowed to cool slowly to room temperature. Colorless X-ray quality crystals were isolated from a white fluffy gel. Yield: 6.2 mg (31%).

X-Ray Crystallography. Diffraction data for **1**, **2·MeCN**, and **3·2MeCN** were collected on a Bruker SMART CCD diffractometer, and data for **bpa**, **4**, and **5** were collected on a Nonius Kappa-CCD diffractometer; both had graphite-monochromated Mo–K α ($\lambda = 0.71073$ Å) radiation. Intensities were corrected for Lorentz-polarization effects,¹⁵ and a multiscan absorption correction was applied except to the data for **bpa**, **4**, and **5**.¹⁶ The structures were solved by direct methods (SHELXS¹⁷ or SIR-97¹⁸) and refined on *F*² using all data by full-matrix least-squares procedures (SHELXL 97¹⁷). All calculations were performed using the WinGX interface.¹⁹ Crystallographic data for the six structures are listed in Table 1.

(15) (a) *SAINTE V4, Area Detector Control and Integration Software*; Siemens Analytical X-ray Systems Inc.: Madison, WI, 1996. (b) Otwinowski, Z.; Minor, W. In *Methods in Enzymology: Macromolecular Crystallography Part A*; Carter, C. W., Jr., Sweet, R. M., Eds.; Academic Press: 1997; Vol. 276, pp 307–326.

(16) Sheldrick, G. M. *SADABS, Program for Absorption Correction*; University of Göttingen: Göttingen, Germany, 1996.

(17) Sheldrick, G. M. *SHELXS and SHELXL*; Institut für Anorganische Chemie der Universität: Göttingen, Germany, 1998.

(18) Altomare, A.; Burla, M. C.; Camalli, M.; Cascarano, G. L.; Giacovazzo, C.; Guagliardi, A.; Moliterni, A. G. G.; Polidori, G.; Spagna, R. *J. Appl. Crystallogr.* **1999**, *32*, 115–119.

(19) Farrugia, L. J. *J. Appl. Crystallogr.* **1999**, *32*, 837–838.

Results and Discussion

Structure of bpa. Colorless X-ray quality crystals were grown as byproducts in the crystallization of several of the complexes. X-ray structural analysis showed the **bpa** molecules to have crystallized in the noncentrosymmetric, orthorhombic space group $P2_1ca$. The asymmetric unit of the structure was found to consist of a single molecule of **bpa** (Figure 1). The pyridine rings were arranged in a fashion similar to the form calculated by Benedix and Hennig,²⁰ although the ring twists differed somewhat. One pyridine ring was twisted at 14.0° and the other at 26.1° relative to the C–N_{amine}–C plane, with an angle of 39.1° between the two ring planes. Benedix and Hennig had also calculated the theoretical C–N_{amine}–C angle as 126° and this too differed slightly from the angle observed in this structure ($128.08(16)^\circ$). These differences, however, are relatively minor, and are most likely due to packing forces present in the solid state.

Despite the presence of the pyridine rings in the **bpa** molecules, no π – π interactions shorter than 4.53 \AA were found in the structure.²¹ The molecules were held together by three sets of interactions. The first of these was a series of strong hydrogen bonds formed between the amine N–H and one N_{py} of an adjacent molecule of **bpa**. The N–H...N distance was found to be 1.90 \AA , with a N...N distance of 2.89 \AA . The N–H...N angle of 176° led to this series of hydrogen bonds being defined as linear.²² The hydrogen-bonded **bpa** molecules formed one-dimensional chains running along the crystallographic c -axis. Two other sets of weaker interactions led to the overall formation of a weakly interacting three-dimensional system. These interactions were both edge-to-face C–H... π interactions, with C–H...centroid distances of 2.76 and 2.78 \AA and corresponding C...centroid distances of 3.52 and 3.54 \AA . These distances were close to the conventional van der Waals limit, but C–H... π interactions have been suggested to be effective at distances beyond this limit.²³ Molecules of **bpa** of both enantiomers were found to be present in the crystal, with adjacent molecules of **bpa** being of different enantiomers.

The structure of **bpa** has been determined twice previously (CSD, version 5.26).²⁴ However both of these reports were private communications to the CSD. The space group and unit-cell data of these two structures were in agreement with those reported here.

Synthesis and Structure of $\{[\text{Ag}(\text{bpa})(\text{MeCN})](\text{CF}_3\text{SO}_3)\}_\infty$ (1**).** The 1:1 molar reaction of AgCF_3SO_3 in degassed MeCN and **bpa** in degassed MeCN–H₂O (3:1, v/v) was allowed to stir overnight. A white precipitate was obtained

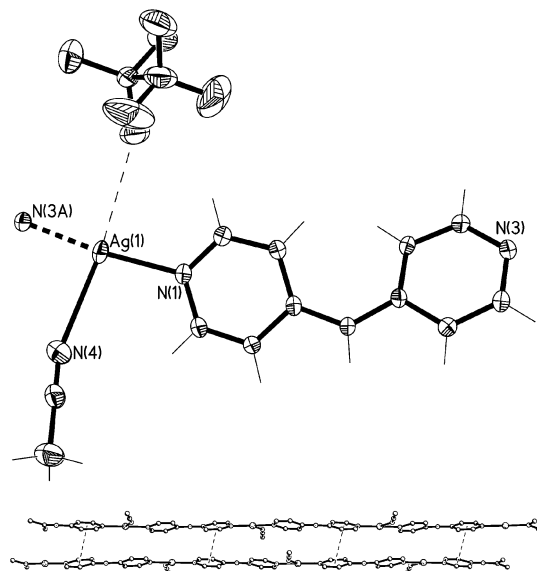


Figure 2. Views of **1**. (top) A view of the **bpa** ligand and Ag^+ coordination environment (crystallographic numbering). Thermal ellipsoids have been drawn at the 50% probability level. The weak interaction between the Ag^+ and an O atom of the CF_3SO_3^- anion is shown dashed. (bottom) View of a centrosymmetric pair of polymeric chains of **1** running along the crystallographic b -axis showing the π – π interactions between symmetry-related pyridine rings. Hydrogen atoms and CF_3SO_3^- anions are omitted. Selected bond lengths (\AA) and angles (deg): N(1)–Ag(1) $2.149(2)$, N(3A)–Ag(1) $2.150(2)$, N(4)–Ag(1) $2.667(3)$; N(1)–Ag(1)–N(3A) $173.58(8)$, N(1)–Ag(1)–N(4) $93.25(9)$, N(3A)–Ag(1)–N(4) $93.17(9)$ (Symmetry code: A $-x + 1, y + 1/2, -z + 1 1/2$).

on concentration of the solution and subsequent addition of diethyl ether. Following precipitation, the complex was found to be insoluble in common organic solvents. Microanalytical data were consistent with the solid having a 1:1 metal-to-ligand ratio. The IR spectrum showed three features in the CF_3SO_3^- stretching region, consistent with the symmetry of the CF_3SO_3^- anion not being significantly changed by the formation of the complex.²⁵ Two further peaks indicative of the presence of the ligand and its incorporation into the complex were also present. Colorless X-ray quality crystals of this complex were grown from the slow diffusion of an *i*PrOH solution of **bpa** layered with MeCN and a H₂O solution of AgCF_3SO_3 .

X-ray structural analysis revealed that this complex formed a one-dimensional zigzag coordination polymer, and crystallized in the monoclinic space group $P2_1/c$. The asymmetric unit consisted of one Ag^+ cation, one complete **bpa** ligand, one CF_3SO_3^- anion, and one molecule of MeCN solvent (Figure 2). The pyridine rings of the **bpa** ligand were somewhat twisted, at an angle of 30.1° with respect to each other. The C–N–C angle across the amine was found to be $129.8(2)^\circ$. Each ligand was bound to two symmetry-related, three-coordinate Ag^+ ions via the N_{py} donors. The Ag^+ ions in turn coordinated to one further **bpa** ligand and one solvent MeCN molecule, leading to a N_{py}–N_{py}–N_{MeCN} coordination environment, with T-shaped stereochemistry. The angles across the Ag^+ ion between the two pyridine N atoms and between each pyridine N atom and the MeCN N atom were

(20) Benedix, R.; Hennig, H. Z. Chem. **1984**, *24*, 303–304.

(21) Janiak, C. Dalton Trans. **2000**, 3885.

(22) (a) Jeffrey, G. A.; Saenger, W. *Hydrogen Bonding in Biological Structures*; Springer-Verlag: Berlin, 1991; p 20. (b) Jeffrey, G. A.; Maluszynska, H.; Mitra, J. Int. J. Biol. Macromol. **1985**, *7*, 336–348.

(23) (a) Nishio, M. CrystEngComm **2004**, *6*, 130–158. (b) Umezawa, Y.; Tsuboyama, S.; Honda, K.; Uzawa, J.; Nishio, M. Bull. Chem. Soc. Jpn. **1998**, *71*, 1207–1213. (c) Nishio, M.; Umezawa, Y.; Hirota, M.; Takeuchi, Y. Tetrahedron **1995**, *51*, 8665–8701.

(24) Allen, F. H.; Davies, J. E.; Galloy, J. J.; Johnson, O.; Kennard, O.; Macrae, C. F.; Mitchell, E. M.; Mitchell, G. F.; Smith, J. M.; Watson, D. G. J. Chem. Inf. Comput. Sci. **1991**, *31*, 187–204.

(25) Socrates, G. *Infrared and Raman Characteristic Group Frequencies*; John Wiley and Sons Ltd.: Chichester, U.K., 2001.

173.57(8), 93.26(9), and 93.17(9)°, respectively. This T-shaped geometry for Ag^I has been found to occur less frequently than the trigonal planar geometry;²⁶ also, three-coordinate Ag^I compounds have been found to be significantly less common than two-coordinate.²⁷ The planes of the pyridine rings coordinated to the same Ag^I ion were twisted by 32.4° with respect to each other.

The Ag–N_{py} bond distances were found to be short, and at the lower end of the range (2.14–2.40 Å) for similar three-coordinate Ag–N_{py} systems found in a search of the CSD.²⁴ In contrast, the MeCN–Ag bond distance was long and just outside the range of values (2.09–2.62 Å) for similar systems. The CF₃SO₃[–] anion was positioned correctly for coordination to Ag^I by an O donor, which would have given rise to a description of the geometry of the Ag^I as very distorted square planar (Figure 2). This stereochemistry is considered to be uncommon for the Ag^I ion, about the same number of examples being found for discrete²⁸ and coordination polymeric systems.²⁹ However, analysis using PLATON³⁰ indicated the CF₃SO₃[–] anion to be nonbonding, resulting in description of the coordination geometry as T-shaped. The Ag···O distance of 3.029(2) Å was longer than the longest reported Ag–O distance (2.96 Å) for a bound CF₃SO₃[–] anion in a search of the CSD.²⁴ The distance was, however, still significantly shorter than the sum (3.20 Å) of the van der Waals radii,³¹ suggesting that an interaction

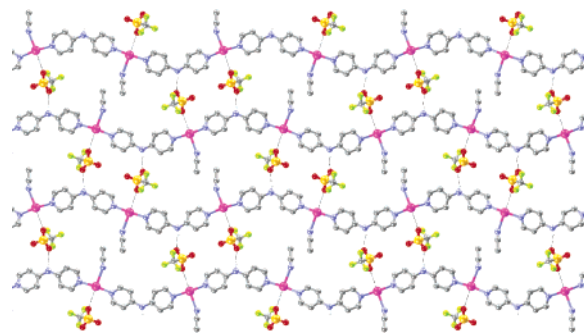


Figure 3. View of a two-dimensional sheet of **1**, lying in the (–1 0 2) plane, formed by interaction of the one-dimensional polymer chains with the CF₃SO₃[–] anions. Hydrogen atoms not involved in hydrogen bonding are omitted (Ag, pink; N, blue; C, gray; H, white; F, green; S, yellow; O, red).

may exist. The interactions of the anion were found to be consistent with the interpretation of the IR spectrum of the complex.

The one-dimensional zigzag polymer chain propagated along the *b*-axis (Figure 2). It did not contain a center of symmetry, and as such was formed by a simple symmetry translation along the *b*-axis. Adjacent parallel chains were related to each other in a centrosymmetric fashion, resulting in an offset between symmetry-related Ag^I ions of 5.5149–(5) Å. Each chain contained **bpa** ligands of only one enantiomer, meaning that the individual chains were chiral. However, because of the centrosymmetric relationship between adjacent chains, an overall achiral structure resulted. There were several significant interactions involving the CF₃SO₃[–] anion that linked adjacent polymer chains into two-dimensional sheets in the (–1 0 2) plane. First, there was a set of hydrogen-bonding interactions between one O atom of the CF₃SO₃[–] anion and the amine N–H of an adjacent chain (Figure 3). The CF₃O₂S–O···H–N distance was 2.03 Å, with a corresponding O···N separation of 2.88 Å. The angle O···H–N was 173°, leading to a description of this interaction as a linear hydrogen bond.²² Second, one O atom of the CF₃SO₃[–] anion was also able to interact with both the Ag^I anion and a H atom of the pyridine ring bound to that Ag^I (Figure 3). The CF₃O₂S–O···Ag distance was 3.03 Å and the CF₃O₂S–O···H–C distance was 2.51 Å, with a corresponding O···C separation of 3.32 Å. Adjacent chains in the (1 0 0) plane were also able to interact to form weakly linked two-dimensional sheets by π–π interactions between symmetry-related pyridine rings, with a centroid–centroid distance of 3.59 Å (Figure 2).²¹ The interaction of the one-dimensional coordination polymers via these hydrogen-bonding and Ag^I–anion interactions led to the formation of a two-dimensional supramolecular array (Figure 3),² this being extended into three dimensions by the weaker electrostatic and π–π interactions. The structure was found to not be porous, with no residual solvent accessible volume and a packing index of 0.74, as calculated using PLATON.³⁰

Synthesis and Structure of {[Ag(bpa)](PF₆)·MeCN}_∞ (2·MeCN). The 1:1 molar reaction of AgPF₆ and **bpa** in degassed MeCN–H₂O (3:1, v/v) was allowed to stir overnight. A white precipitate was obtained on concentration of

- (26) Venkataraman, D.; Du, Y.; Wilson, S. R.; Hirsch, K. A.; Zhang, P.; Moore, J. S. *J. Chem. Educ.* **1997**, *74*, 915–918.
- (27) (a) Munakata, M.; Wu, L. P.; Kuroda-Sowa, T. *Adv. Inorg. Chem.* **1998**, *46*, 173–303. (b) Cotton, F. A.; Wilkinson, G.; Murillo, C. A.; Bochmann, M.; Grimes, R. *Advanced Inorganic Chemistry*, 6th ed.; John Wiley and Sons Ltd.: Chichester, U.K., 1999; p 1085. (c) Lancashire, R. J. In *Comprehensive Coordination Chemistry*; Wilkinson, G., Gillard, R. D., McCleverty, J. A., Eds.; Pergamon Press: Oxford, U.K., 1987; Vol. 5, pp 775–850.
- (28) (a) Hou, L.; Li, D.; Yin, Y.; Wu, T.; Ng, S. W. *Acta Crystallogr., Sect. E* **2004**, *60*, m1106–m1107. (b) Reger, D. L.; Gardinier, J.; Smith, M. D. *Polyhedron* **2004**, *23*, 291–299. (c) Reger, D. L.; Gardinier, J.; Smith, M. D. *Inorg. Chem.* **2004**, *43*, 3825–3832. (d) Constable, E. C.; Housecroft, C. E.; Kariuki, B. M.; Kelly, N.; Smith, C. B. *Inorg. Chem. Commun.* **2002**, *5*, 199–202. (e) Carmona, D.; Viguri, F.; Lahoz, F. J.; Oro, L. A. *Inorg. Chem.* **2002**, *41*, 2385–2388. (f) Heyduk, A. F.; Krodel, D. J.; Meyer, E. E.; Nocera, D. G. *Inorg. Chem.* **2002**, *41*, 634–635. (g) Chen-jie, F.; Chun-ying, D.; Hong, M.; Cheng, H.; Qing-jin, M.; Yong-jiang, L.; Yu-hua, M.; Zhe-ming, W. *Organometallics* **2001**, *20*, 2525–2532. (h) Chen, Z.; Wang, R.-J.; Dilks, K. J.; Li, J. *J. Solid State Chem.* **1999**, *147*, 132–139. (i) Constable, E. C.; Edwards, A. J.; Haire, G. R.; Hannon, M. J.; Raithby, P. R. *Polyhedron* **1998**, *17*, 243–253. (j) Arduengo, A. J., III; Diasand, H. V. R.; Calabrese, J. C. *J. Am. Chem. Soc.* **1991**, *113*, 7071–7072. (k) Nasielski, J.; Nasielski-Hinkens, R.; Heilporn, S.; Rypens, C.; Declercq, J. P. *Bull. Soc. Chim. Belg.* **1988**, *97*, 983–992. (l) Fritchie, C. J., Jr. *J. Biol. Chem.* **1972**, *247*, 7459–7464.
- (29) (a) Hanton, L. R.; Young, A. G. *Cryst. Growth Des.* **2006**, *6*, 833–835. (b) Amore, J. J. M.; Hanton, L. R.; Spicer, M. D. *Supramol. Chem.* **2005**, *17*, 557–565. (c) Chowdhury, S.; Drew, M. G. B.; Datta, D. *New J. Chem.* **2003**, *27*, 831–835. (d) Suenaga, Y.; Kitamura, K.; Kuroda-Sowa, T.; Maekawa, M.; Munakata, M. *Inorg. Chim. Acta* **2002**, *328*, 105–110. (e) Patra, G. K.; Goldberg, I. *J. Chem. Soc., Dalton Trans.* **2002**, 1051–1057. (f) Ino, I.; Zhong, J.; Munakata, M.; Kuroda-Sowa, T.; Maekawa, M.; Suenaga, Y.; Kitamori, Y. *Inorg. Chem.* **2000**, *39*, 4273–4279. (g) Hong, M.; Zhao, Y.; Su, W.; Cao, R.; Fujita, M.; Zhou, Z.; Chan, A. S. C. *Angew. Chem., Int. Ed.* **2000**, *39*, 2468–2470. (h) Smith, G.; Cloutt, B. A.; Byriel, K. A.; Kennard, C. H. L. *Aust. J. Chem.* **1997**, *50*, 741–746. (i) Carlucci, L.; Ciani, G.; Proserpio, D. M.; Sironi, A. *Angew. Chem., Int. Ed.* **1995**, *34*, 1895–1898. (j) Bing, X.; Dong, C.; Wenxia, T.; Kaibei, Y.; Zhongyuan, Z. *Acta Crystallogr., Sect. C* **1991**, *47*, 1805–1808.
- (30) Spek, A. L. *PLATON*; *J. Appl. Crystallogr.* **2003**, *36*, 7–13.
- (31) Bondi, A. *J. Phys. Chem.* **1964**, *68*, 441–451.

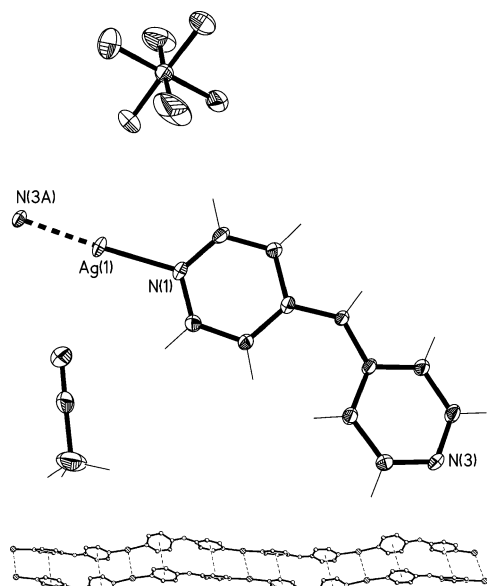


Figure 4. Views of **2-MeCN**. (top) View of the **bpa** ligand and Ag^{I} coordination environment (crystallographic numbering). Thermal ellipsoids have been drawn at the 50% probability level. (bottom) View of a pair of strongly interacting one-dimensional polymer chains running along the [2 0 1] diagonal axis showing the $\text{Ag}\cdots\text{Ag}$ and $\pi\cdots\pi$ interactions. Hydrogen atoms, PF_6^- anions, and MeCN solvent molecules are omitted. Selected bond lengths (\AA) and angles (deg): $\text{N}(1)-\text{Ag}(1)$ 2.125(2), $\text{N}(3\text{A})-\text{Ag}(1)$ 2.130(2); $\text{N}(1)-\text{Ag}(1)-\text{N}(3\text{A})$ 174.03(9) (Symmetry code: $A\ x, -y, z + 1/2$).

the solution and subsequent addition of diethyl ether. Following precipitation, the complex was found to be insoluble in common organic solvents. Microanalytical data were consistent with the solid having a 1:1 metal-to-ligand ratio. The IR spectrum showed one feature in the PF_6^- stretching region, consistent with the symmetry of the PF_6^- anion not being significantly changed by the formation of the complex.²⁵ Also present were peaks indicative of the ligand. Colorless X-ray quality crystals of this complex were grown from the slow diffusion of an *i*PrOH solution of **bpa** layered with MeCN and a H_2O solution of AgPF_6 .

X-ray structural analysis revealed that this complex formed a one-dimensional zigzag coordination polymer and crystallized in the monoclinic space group $P2_1/c$. The asymmetric unit consisted of one Ag^{I} cation, one complete **bpa** ligand, one PF_6^- anion, and one molecule of MeCN solvent (Figure 4). The pyridine rings of the **bpa** ligand were slightly twisted, at an angle of 22.9° with respect to each other. The C–N–C angle across the amine was found to be $131.8(2)^\circ$. Each ligand was bound to two symmetry-related, two-coordinate Ag^{I} ions via the N_{py} donors. The Ag^{I} ions in turn coordinated to one further **bpa** ligand, leading to a $\text{N}_{\text{py}}\text{N}_{\text{py}'}$ coordination environment with approximately linear stereochemistry (angle $\text{N}_{\text{py}}-\text{Ag}-\text{N}_{\text{py}'}$ = $174.03(9)^\circ$). The pyridine rings bound to the same Ag^{I} ion were found to be close to coplanar, with an angle between them of only 13.9° . The **bpa** ligands in each chain consisted of alternating enantiomers, leading to an overall nonchiral structure.

The $\text{Ag}-\text{N}_{\text{py}}$ bond distances were found to be short, and at the lower end of the range (2.10–2.23 \AA) for similar two-coordinate $\text{Ag}-\text{N}_{\text{py}}$ systems as determined by a search of

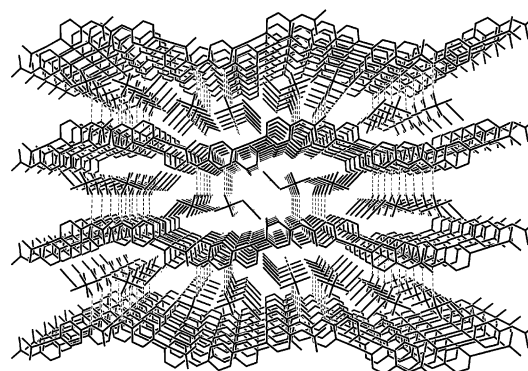


Figure 5. View down the crystallographic a -axis of the packing of two-dimensional sheets of **2-MeCN** showing the anions and solvent molecules interacting with adjacent two-dimensional π -stacked sheets of the complex. Hydrogen atoms are omitted.

the CSD.²⁴ The MeCN solvent molecule was positioned correctly for coordination to Ag^{I} via its N donor (Figure 4). This would have given rise to a description of the geometry of the Ag^{I} as T-shaped. However, analysis using PLATON³⁰ indicated the MeCN solvent to be nonbonding. The $\text{Ag}\cdots\text{N}$ distances of 2.914(3) \AA was longer than the longest reported $\text{Ag}-\text{N}$ distance (2.73 \AA) for a bound MeCN molecule in a search of the CSD.²⁴ The distance was still shorter than the sum (3.25 \AA) of the van der Waals radii,³¹ suggesting the existence of a weak interaction.

The one-dimensional zigzag polymer chain that was formed propagated along the [2 0 1] diagonal axis. It did not contain a center of symmetry, and as such was formed by a simple symmetry translation along the [2 0 1] axis. Polymeric chains formed pairs, interacting through Ag^{I} ions and $\pi-\pi$ stacking (Figure 4). Both the pyridine rings and Ag^{I} ions in the paired chains were in exact register with each other. The $\text{Ag}\cdots\text{Ag}$ distance was 3.2669(5) \AA , and the centroid–centroid distance was 3.66 \AA with an angle between the pyridine rings of 13.9° .²¹ This $\text{Ag}\cdots\text{Ag}$ distance was within the range of previously recognized $\text{Ag}\cdots\text{Ag}$ interactions (2.80–3.37 \AA),³² although toward the high end and was less than the sum (3.40 \AA)³¹ of the van der Waals radii, suggesting a weak interaction was occurring. Adjacent pairs of chains were related to each other in a centrosymmetric fashion, resulting in **bpa** ligands of adjacent chains being offset from each other by half of a ligand molecule. Adjacent pairs of chains in the (0 1 0) plane were linked together to form undulating two-dimensional sheets by three $\pi-\pi$ interactions between pyridine rings (Figure 5), with centroid–centroid distances in the range 3.40–4.06 \AA .²¹ These pyridine rings were close to parallel, with the angle between them ranging from 0.0– 13.5° .

The PF_6^- anions were held firmly in place by hydrogen-bonding interactions. Two separate F atoms of the PF_6^- anion were able to form hydrogen bonds with the same amine N–H. The $\text{F}_3\text{P}-\text{F}\cdots\text{H}-\text{N}$ distances were 2.15 and 2.50 \AA ,

(32) (a) Gimeno, M. C.; Laguna, A. In *Comprehensive Coordination Chemistry II*; McCleverty, J. A., Meyer, T. J., Eds.; Elsevier Pergamon: Boston, 2004; Vol. 6, pp 911–1145. (b) Tong, M.-L.; Chen, X.-M.; Ye, B.-H.; Ji, L.-N. *Angew. Chem., Int. Ed.* **1999**, *38*, 2237–2240. (c) Pyykkö, P. *Chem. Rev.* **1997**, *97*, 597–636.

with corresponding F[⋯]N separations of 2.93 and 3.28 Å. Both F[⋯]H–N angles were 151° and, combined with a F[⋯]H[⋯]F angle of 58°, led to a description of this interaction as a three-center, bifurcated hydrogen bond.²² In contrast to **1**, there were no strong interactions between the two-dimensional sheets. However, both the PF₆[−] anion and the MeCN molecule were able to form weak interactions between sheets, forming a three-dimensional array (Figure 5). The PF₆[−] anion formed two types of weak interactions. The first of these was a F₅P–F[⋯]Ag interaction at a distance of 3.22 Å. The other type was a series of F₅P–F[⋯]H–C interactions with both pyridine and MeCN hydrogen atoms, at F[⋯]H distances of 2.38–2.46 Å, with corresponding F[⋯]C separations in the range 3.05–3.37 Å. The weak interactions of the anion were found to be consistent with the interpretation of the IR spectrum of the complex.

The structure did not display pores as such; however, the two-dimensional cationic sheets that formed had a separation of approximately 5 Å, which was occupied by the anions and solvent molecules. The volume of the gaps occupied by the MeCN solvent molecules was 17.8% of the unit cell volume, which led to the framework having a packing index of 0.64.³⁰ When the complete structure, including solvent, was considered, the gaps were found to be occupied, leading to the structure having no residual accessible volume and a packing index of 0.74.³⁰

Synthesis and Structure of {[Ag(bpa)](ClO₄)·2MeCN}_∞ (3·2MeCN). The 1:1 molar reaction of AgClO₄ and **bpa** in degassed MeCN/H₂O (3:1, v/v) was allowed to stir overnight. The white solid that precipitated was isolated in reasonable yield and gave microanalytical data consistent with a 1:1 metal-to-ligand ratio. The complex was found to be insoluble in common organic solvents. The IR spectrum showed one feature in the ClO₄[−] stretching region, a strong peak at 1084 cm^{−1}, consistent with the symmetry of the ClO₄[−] anion not being significantly changed by the formation of the complex.²⁵ Also present were peaks indicative of the ligand at 3416 and 528 cm^{−1}. Colorless plate-shaped X-ray quality crystals of this complex were grown from the slow diffusion of a 2,2,2-trifluoroethanol solution of **bpa** layered with MeNO₂ and a MeCN solution of AgClO₄. These crystals were seen to slowly lose solvent and, as a result, crystallinity when removed from the mother liquor.

X-ray structural analysis revealed that this complex formed a one-dimensional zigzag coordination polymer and crystallized in the monoclinic space group *P*2₁/*c*. The asymmetric unit consisted of two Ag^I cations, two complete **bpa** ligands, two PF₆[−] anions, and four molecules of MeCN solvent (Figure 6). The pyridine rings in each of the independent **bpa** ligands were somewhat twisted, at angles of 26.0 and 38.4° with respect to each other. The C–N–C angles across the independent amines were found to be 127.9(11) and 132.1(11)°. Each ligand was bound to two independent, two-coordinate Ag^I ions via the N_{py} donors. The Ag^I ions in turn coordinated to one further **bpa** ligand, leading to a N_{py}N_{py}' coordination environment for both Ag^I ions, with effectively linear stereochemistry (angle N_{py}–Ag–N_{py}' = 178.1(4) and 179.0(4)°). The independent pyridine rings were found to

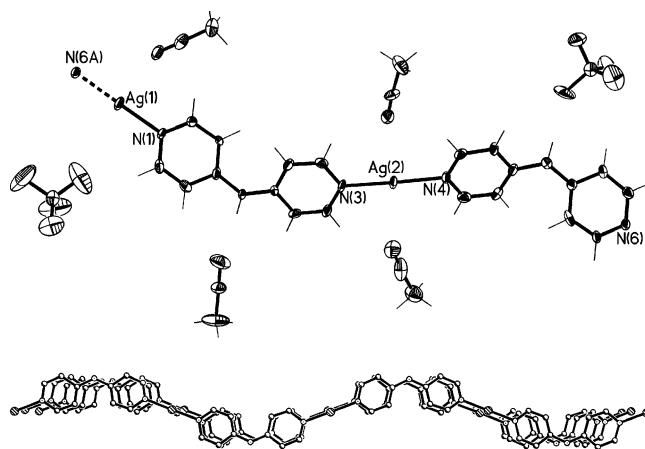


Figure 6. Views of **3·2MeCN**. (top) A view of the **bpa** ligands and Ag^I coordination environments (crystallographic numbering). Thermal ellipsoids have been drawn at the 50% probability level. (bottom) View showing the almost exact register of adjacent chains running along the crystallographic *b*-axis and giving rise to undulating two-dimensional sheets. Hydrogen atoms, ClO₄[−] anions, and MeCN solvent molecules are omitted. Selected bond lengths (Å) and angles (deg): N(1)–Ag(1) 2.127(10), N(3)–Ag(2) 2.141(10), N(4)–Ag(2) 2.183(9), N(6A)–Ag(1) 2.148(10); N(1)–Ag(1)–N(6A) 179.0(4), N(3)–Ag(2)–N(4) 178.1(4) (Symmetry code: *A* *x*, *y* + 1, *z*).

be approximately coplanar across the Ag^I ions, with ring twists of 5.8 and 9.0°. The Ag–N_{py} bond distances were found to be close to the middle of the range (2.10–2.23 Å) for similar two-coordinate Ag–N_{py} systems found in a search of the CSD.²⁴ Three of the MeCN solvent molecules were positioned correctly for coordination to the Ag^I ions via N donors, which would have given rise to a description of the geometry of one of the Ag^I ions as T-shaped and the other as very distorted tetrahedral (Figure 6). However, analysis using PLATON³⁰ indicated all the MeCN solvent molecules to be nonbonding. The shortest Ag[⋯]N distances of 2.800–(13) Å was longer than the longest reported Ag–N distance (2.73 Å) for a bound MeCN molecule in a search of the CSD.²⁴ The distance was still shorter than the sum (3.25 Å) of the van der Waals radii,³¹ suggesting that a weak interaction may exist.

The one-dimensional zigzag polymer chain propagated along the *b*-axis (Figure 6). It did not contain a center of symmetry, and as such was formed by a simple symmetry translation along *b*. The two **bpa** ligands in the asymmetric unit were of different enantiomers, thus the individual polymer chains were not chiral. Adjacent chains were related to each other in a centrosymmetric fashion, with the **bpa** ligands of adjacent chains almost in exact register with each other, and so able to π -stack. The chains in the (0 0 1) plane were linked together to form undulating two-dimensional sheets by a number of interactions (Figure 6). The strongest of these were two sets of hydrogen bonds. These were formed between each of the two independent amine N–H, one O atom of a ClO₄[−] anion, and the N atom of a MeCN solvent molecule (Figure 7). Each amine N–H interacted with both a ClO₄[−] anion and a MeCN solvent molecule and formed hydrogen bonded sheets. The O₃Cl–O[⋯]H–N distances were 2.43 and 2.56 Å, with corresponding O[⋯]N separations of 3.21 and 3.24 Å. The H₃C–C≡N[⋯]H–N distances were 2.36

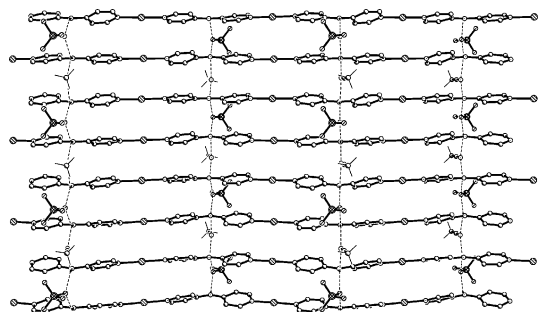


Figure 7. View of the network of hydrogen bonds between adjacent chains in **3·2MeCN** forming two-dimensional sheets in the (0 0 1) plane. Pyridine rings can also be seen positioned to π -stack. Hydrogen atoms of the pyridine rings, MeCN solvent molecules, and ClO_4^- anions not involved in hydrogen bonding are omitted.

and 2.58 Å, with corresponding $\text{N}\cdots\text{N}$ separations of 3.02 and 3.03 Å. The angles for the two hydrogen-bonding systems were similar: for one, the $\text{O}\cdots\text{H}-\text{N}$ angle was 135° , the $\text{N}\cdots\text{H}-\text{N}$ angle was 133° , and the $\text{O}\cdots\text{H}\cdots\text{N}$ angle was 92° ; for the other, the $\text{O}\cdots\text{H}-\text{N}$ angle was 148° , the $\text{N}\cdots\text{H}-\text{N}$ angle was 112° , and the $\text{O}\cdots\text{H}\cdots\text{N}$ angle was 100° . In both cases, the combination of the angles led to a description of these interactions as three-center, bifurcated hydrogen bonds.³¹ This hydrogen-bonding motif led to both ClO_4^- anions and MeCN solvent molecules bridging adjacent chains by hydrogen bonding in an alternating pattern (Figure 7). This is an unusual motif for hydrogen-bonded MeCN, with very few examples having been identified,³³ none of which give rise to polymeric structures.

The other significant interactions were strong $\pi-\pi$ interactions between both pyridine rings and their independent counterparts in adjacent chains, with centroid-centroid distances of 3.65 and 3.66 Å.²¹ These pyridine rings were close to parallel, with the angle between them being either 5.8 or 9.0° . Because of these strong interchain interactions, the Ag^{I} ions of adjacent chains were brought into proximity, with $\text{Ag}\cdots\text{Ag}$ separations of 3.568(2) and 3.646(2) Å. However, the Ag^{I} ions were found to not be interacting, as the separation between them was greater than the sum (3.40 Å) of the van der Waals radii.³¹

Both the ClO_4^- anion and the MeCN solvent molecules were also able to make several types of weaker interactions. For the ClO_4^- anion, the first of these was a $\text{O}_3\text{Cl}-\text{O}\cdots\text{Ag}$ interaction at a distance of 3.49 Å. The other type was a series of $\text{O}_3\text{Cl}-\text{O}\cdots\text{H}-\text{C}$ interactions with both pyridine and MeCN hydrogen atoms, at $\text{O}\cdots\text{H}$ distances of 2.33–2.51 Å, with corresponding $\text{O}\cdots\text{C}$ separations in the range 3.10–3.50 Å. The interactions of the anion were found to be consistent with the interpretation of the IR spectrum of the complex. The MeCN molecules also interacted weakly with the Ag^{I} ion, giving $\text{H}_3\text{C}-\text{C}\equiv\text{N}\cdots\text{Ag}$ distances of 2.83–3.49 Å. In contrast to **1**, and in common with **2·MeCN**, the combination of hydrogen bonding and π -stacking led to two-dimensional sheets rather than a three-dimensional network.

However, the weak interactions mediated by the ClO_4^- anion and the MeCN molecules led to the formation of a three-dimensional supramolecular array in a manner similar to that occurring in **2·MeCN**.

The structure did not display pores as such, but the two-dimensional cationic sheets that formed had a separation of approximately 8 Å, which was occupied by the anions and solvent molecules. The volume of the gaps occupied by the MeCN solvent molecules was 27.1% of the unit cell volume, which led to the cationic framework having a packing index of 0.57.³⁰ When the complete structure, including solvent, was considered, the gaps were found to be occupied leading to the structure having no residual accessible volume and a packing index of 0.76.³⁰

Synthesis and Structure of $\{[\text{Ag}(\text{bpa})](\text{ClO}_4)\}_\infty$ (4**).** The hydrothermal, 1:1 molar reaction of AgClO_4 and **bpa** was allowed to proceed in a sealed Pyrex tube, protected by a steel blast tube, at 120°C for 64 h. No problems were encountered because of very small amounts of reactants being used and precautions taken to minimize the damage in the event of an explosion. The reaction mixture was then allowed to cool slowly to room temperature, and gave X-ray quality crystals as colorless prisms in low yield, suspended in a fluffy white solid. Because of the scarcity of crystalline material, the only analysis carried out on this material was X-ray diffraction. In contrast to the crystals of **3·2MeCN**, these crystals were seen to not lose solvent.

X-ray structural analysis revealed that this complex formed a one-dimensional single-stranded helical coordination polymer, which crystallized in the hexagonal space group $P6_5-22$. As was necessary for this enantiomorphic space group, only the *M* enantiomer of the helix was observed; however, the refined Flack *x*-parameter³⁴ of the structure (0.55(5)) indicated that racemic twinning had occurred. In this complex, the chirality of the **bpa** ligands led to the formation of a helical complex, in contrast to the previously seen zigzag coordination polymers. As the **bpa** ligand existed as a racemate in solution, the crystal used for data collection was most likely the result of conglomerate crystallization.

The asymmetric unit of the complex consisted of half of a Ag^{I} cation, half of a **bpa** ligand, and half of a ClO_4^- anion (Figure 8). Each ligand was bound to two symmetry-related, two-coordinate Ag^{I} ions via the N_{py} donors. The pyridine rings of each **bpa** ligand were significantly twisted, with an angle of 50.3° between them. The $\text{C}-\text{N}-\text{C}$ angle across the amine was found to be $125.9(4)^\circ$. The Ag^{I} ions in turn coordinated to one further **bpa** ligand, leading to a $\text{N}_{\text{py}}\text{N}_{\text{py}'}$ coordination environment for the Ag^{I} ions, with approximately linear stereochemistry (angle $\text{N}_{\text{py}}-\text{Ag}-\text{N}_{\text{py}'} = 174.22-(15)^\circ$). However despite this, pyridine rings bound to the same Ag^{I} ion were found to also be significantly twisted with respect to each other, with an angle between rings of 58.5° . The $\text{Ag}-\text{N}_{\text{py}}$ bond distances were seen to be short and at the lower end of the range (2.10–2.23 Å) for similar

(33) (a) Lah, N.; Giester, G.; Segedin, P.; Murn, A.; Podlipnik, K.; Leban, I. *Acta Crystallogr., Sect. C* **2001**, *57*, 546–548. (b) Wang, Y.; Jian, F.-F.; Yang, X.-J.; Lu, L.-D.; Wang, X.; Fun, H.-K.; Chantrapromma, S.; Razak, I. A. *Acta Crystallogr., Sect. E* **2001**, *57*, o312–o314.

(34) (a) Bernardinelli, G.; Flack, H. D. *Acta Crystallogr., Sect. A* **1985**, *41*, 500–511. (b) Flack, H. D. *Acta Crystallogr., Sect. A* **1983**, *39*, 876–881.

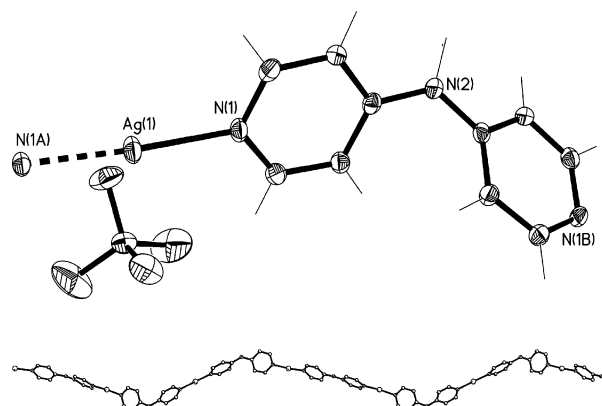


Figure 8. Views of **4**. (top) View of the **bpa** ligand and Ag^I coordination environment (crystallographic numbering). Both symmetry disordered H atoms bound to N(2) are shown. Thermal ellipsoids have been drawn at the 50% probability level. (bottom) View of a single strand of the helical chain of **4** propagating along the crystallographic *c*-axis. Hydrogen atoms and ClO₄⁻ anions are omitted for clarity. Selected bond lengths (Å) and angles (deg): N(1)–Ag(1) 2.113(2), Ag(1)–N(1A) 2.113(2); N(1A)–Ag(1)–N(1) 174.22(15) (Symmetry code: $A - y + 1, -x + 1, -z + 1/6$).

two-coordinate Ag–N_{py} systems found in a search of the CSD.²⁴ Two O atoms of the ClO₄⁻ anion were correctly positioned to chelate to the Ag^I ion, which would have led to a description of the coordination geometry as very distorted tetrahedral (Figure 8). However, analysis using PLATON³⁰ indicated all the ClO₄⁻ anions to be nonbonding. The Ag⋯O distance of 2.9341(1) Å was slightly longer than the longest reported Ag–O distance (2.73 Å) for a chelated ClO₄⁻ anion in a search of the CSD,²⁴ although it was shorter than the longest reported distances for a monodentate coordinated ClO₄⁻ anion (3.094 Å). The distance was also significantly shorter than the sum (3.20 Å) of the van der Waals radii,³¹ which suggested a strong interaction or weak bond might exist.

The helical polymer chain propagated along one of the 3₂ screw axes, parallel to the crystallographic *c*-axis (Figure 8). It had a long pitch of 33.3449(10) Å, equal to the length of the *c*-axis. The helices were found to pack closely together (Figure 9), resulting in the formation of a strongly interacting π -stack. The centroid–centroid distance was 3.56 Å,²¹ with the pyridine rings involved strictly parallel to each other. The helices were further held together in a three-dimensional array by a number of interactions between helical chains and ClO₄⁻ anions in addition to this π -stacking (Figure 10). The ClO₄⁻ anions were able to form a set of hydrogen bonds via two symmetry-related O atoms to interact with the amine N–H. The O₃Cl–O⋯H–N distances were both 2.19 Å, with O⋯N separations of 3.19 Å. The O⋯H–N angles were 128 and 154°, and the O⋯H⋯O angle was 60°. The combination of the angles led to a description of this interaction as a three-center, bifurcated hydrogen bond.²²

The ClO₄⁻ anion was also able to make several types of weaker interactions. The first of these was the O₃Cl–O⋯Ag interaction discussed previously, at a distance of 2.94 Å. The second was a O₃Cl–O⋯ π interaction, with an O⋯centroid distance of 3.20 Å. Interactions between electron-poor π -systems and anions were only recognized recently,³⁵ and in most of the cases, investigations have

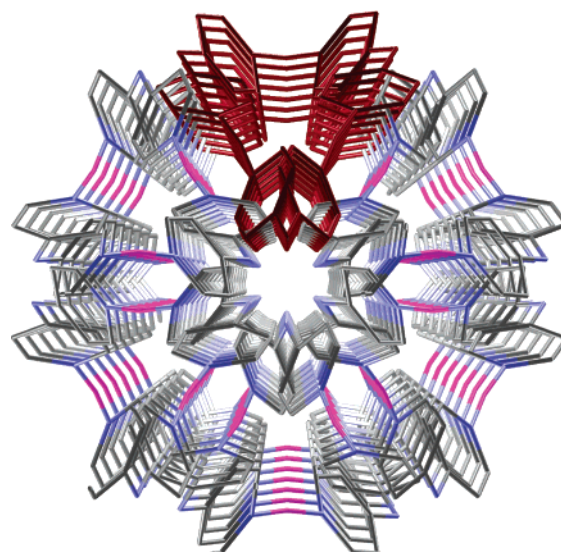


Figure 9. View down the crystallographic *c*-axis showing the close packing of adjacent helices and the resulting lack of free volume in the structure. One helix is highlighted in red. Hydrogen atoms and ClO₄⁻ anions omitted.

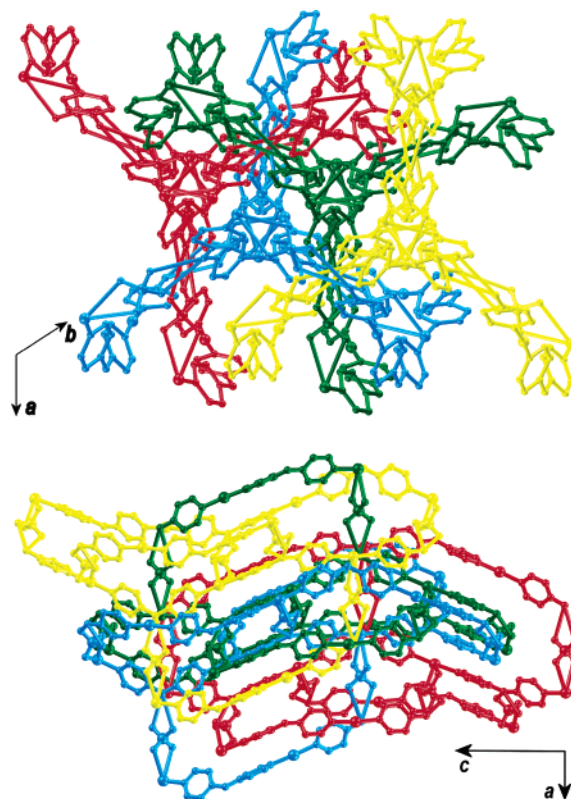


Figure 10. Views of the 4-fold interpenetrated nets of helices of **4**.

involved aromatic systems that have multiple electron-withdrawing substituents. Two recent cases have shown that less electron-deficient π -systems, such as nitrogen-containing heteroaromatic rings, can also interact with anions.³⁶ The O⋯centroid distance of 3.20 Å seen here was shorter than

(35) (a) Quiñero, D.; Garau, C.; Rotger, C.; Frontera, A.; Ballester, P.; Costa, A.; Deyà, P. M. *Angew. Chem., Int. Ed.* **2002**, *41*, 3389–3392. (b) Mascal, M.; Armstrong, A.; Bartberger, M. D. *J. Am. Chem. Soc.* **2002**, *124*, 6274–6276.

the distance of 3.47 Å seen in the only other complex reported as containing a pyridine...anion interaction.^{36b} The other type of interaction involving the ClO_4^- anions was a series of $\text{O}_3\text{Cl}-\text{O}\cdots\text{H}-\text{C}$ interactions with pyridine hydrogen atoms, at $\text{O}\cdots\text{H}$ distances of 2.44–2.50 Å, with corresponding $\text{O}\cdots\text{C}$ separations in the range 3.21–3.30 Å. The interactions of the anion were found to be consistent with the interpretation of the IR spectrum of the complex. The extensive intermolecular interactions, especially the $\pi-\pi$ stacking,³⁷ were most likely responsible for the enantioselection on crystallization, as a crystal made up of just one enantiomer of the helix would pack more efficiently than a racemic mixture of *M* and *P* helices. The structure was not porous, with the ClO_4^- anions residing in small cavities between adjacent helices. This resulted in the structure having no solvent accessible volume, in stark contrast to **3·2MeCN**, and a packing index of 0.77.³⁰ The helices were held together to form four identical, interpenetrating three-dimensional arrays by the two strong interactions involving the ClO_4^- anions (Figure 10).

Synthesis and Structure of $\{[\text{Ag}(\text{bpa})](\text{NO}_3)\}_\infty$ (5**).** The 1:1 molar reaction of AgNO_3 and **bpa** produced a white solid in good yield (78%) that gave microanalytical data consistent with a 1:1 metal-to-ligand ratio. The complex was found to be insoluble in common organic solvents. The IR spectrum showed one feature in the NO_3^- stretching region, a strong peak at 1351 cm^{-1} , which suggested that the NO_3^- anion was not coordinated. Also present were peaks indicative of the ligand, at 3418 and 531 cm^{-1} . Colorless prism-shaped X-ray quality crystals formed at the aqueous–organic interface after the slow diffusion of a $\text{MeCN}-\text{H}_2\text{O}$ solution of **bpa** layered with benzene and a MeCN solution of AgNO_3 . Interestingly, the hydrothermal, 1:1 molar reaction of AgNO_3 and **bpa** carried out in a sealed Pyrex tube at 120°C for 2 days produced crystals that were found to have the same unit-cell dimensions and space group.

X-ray structural analysis revealed that this complex formed a one-dimensional single-stranded helical coordination polymer, which crystallized in the trigonal space group $R32$. Solution and refinement of the structure were carried out using the hexagonal setting of $R32$. In this complex, as in **4**, the chirality of the **bpa** ligands in the solid state led to the formation of a helical complex, in contrast to the previously seen zigzag coordination polymers. Only the *M* enantiomer of the helix was observed in the crystal (Flack parameter $-0.03(9)$).

The asymmetric unit of the complex consisted of half of a Ag^{I} cation, half of a **bpa** ligand molecule, and two NO_3^- anions, one with one-third occupancy and the other with one-sixth (Figure 11). The pyridine rings of each **bpa** ligand were significantly twisted, with an angle of 45.5° between them. The $\text{C}-\text{N}-\text{C}$ angle across the amine was found to be

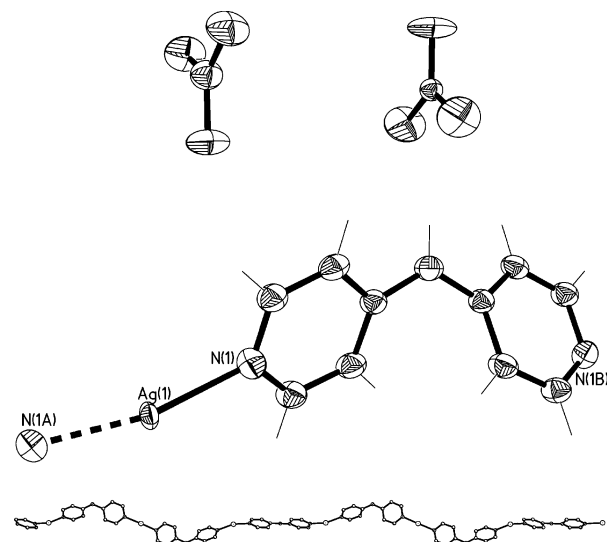


Figure 11. Views of **5**. (top) A view of the **bpa** ligands and Ag^{I} coordination environments (crystallographic numbering). Both partially occupied NO_3^- anions are shown. Thermal ellipsoids have been drawn at the 50% probability level. (bottom) View of a single strand of the helical chain of **5** propagating along the crystallographic *c*-axis. Hydrogen atoms and NO_3^- anions are omitted for clarity. Selected bond lengths (Å) and angles (deg): $\text{Ag}(1)-\text{N}(1)$ 2.163(5), $\text{Ag}(1)-\text{N}(1\text{A})$ 2.163(5); $\text{N}(1)-\text{Ag}(1)-\text{N}(1\text{A})$ 160.8(3) (Symmetry code: $A\ x - y, -y, -z, B\ \frac{1}{3} - x, \frac{2}{3} - x + y, \frac{2}{3} - z$).

$124.3(9)^\circ$. Each ligand was bound via the N_{py} donors to two symmetry-related, two-coordinate Ag^{I} ions with approximately linear geometry (angle $\text{N}_{\text{py}}-\text{Ag}-\text{N}_{\text{py}}' = 161^\circ$). Symmetry-related pyridine rings bound to the same Ag^{I} ion were found to be moderately twisted with respect to each other, with an angle between the pyridine rings of 23.7° . The $\text{Ag}-\text{N}_{\text{py}}$ bond distances fell in the middle of the range (2.10–2.23 Å) for similar two-coordinate $\text{Ag}-\text{N}_{\text{py}}$ systems found in a search of the CSD.²⁴

The helical polymer chain propagated along one of the 3_1 screw axes, parallel to the crystallographic *c*-axis (Figure 11). It had a long pitch of 34.56 Å, equal to the length of the *c*-axis. The helices were found to not pack as closely together as had been seen in **4**, and as a result, the aromatic rings of ligands in neighboring helices were found to be too distant to take part in $\pi-\pi$ interactions, with the shortest distance between centroids being 4.70 Å.²¹ One of the NO_3^- anions formed weak interactions with the Ag^{I} ions. The $\text{Ag}\cdots\text{O}$ distances of 2.88 and 3.05 Å were at the boundary of previously reported $\text{Ag}-\text{O}$ distances (2.25–2.94 Å) for chelated NO_3^- anions, found in a search of the CSD.²⁴ The other NO_3^- was firmly held in place by hydrogen bonds. Three pairs of symmetry-related O atoms of the same NO_3^- anion were able to form hydrogen bonds to three adjacent amines (Figure 12). The $\text{O}_2-\text{N}-\text{O}\cdots\text{H}-\text{N}$ distances were all 2.34 Å, with corresponding $\text{O}\cdots\text{N}$ separations of 3.12 Å. The $\text{O}\cdots\text{H}-\text{N}$ angles of 153° , combined with the $\text{O}\cdots\text{H}\cdots\text{O}$ angle of 54° , led to a description of these interactions as three-centered, bifurcated hydrogen bonds.²² The symmetry of these interactions, despite their strength, confirmed the interpretation of the IR spectrum. The helices were held together to form a three-dimensional array by these hydrogen bonds. These interac-

(36) (a) Garau, C.; Frontera, A.; Quiñero, D.; Ballester, P.; Costa, A.; Deyà, P. M. *J. Phys. Chem. A* **2004**, *108*, 9423–9427. (b) de Hoog, P.; Gamez, P.; Mutikainen, I.; Turpeinen, U.; Reedijk, J. *Angew. Chem., Int. Ed.* **2004**, *43*, 5815–5817. (c) Demeshko, S.; Dechert, S.; Meyer, F. *J. Am. Chem. Soc.* **2004**, *126*, 4508–4509.

(37) Matsumoto, T.; Kasai, T.; Tatsumi, K. *Chem. Lett.* **2002**, *31*, 346–347.

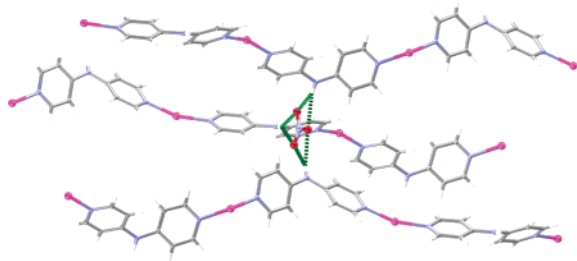


Figure 12. View of the three pairs of symmetry-related N–H...O H-bonds that establish the topological net (Ag, pink; N, blue; C, gray; O, red; H, white).

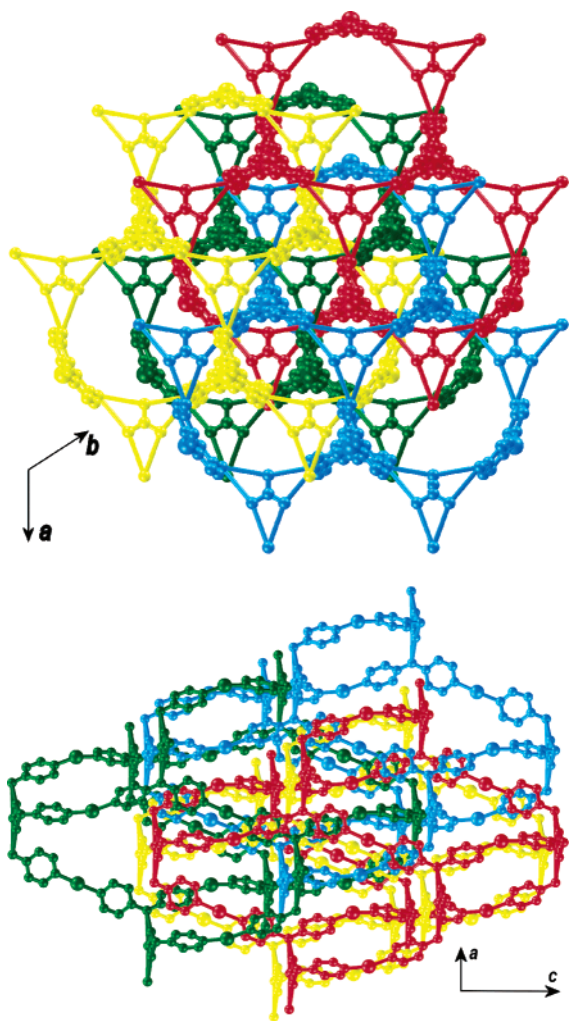


Figure 13. Views of the 4-fold interpenetrated three-dimensional hydrogen bonded networks of helices of **5**.

tions were also reinforced by a number of weaker interactions involving the NO₃[−] anions. These consisted of O₂–N–O...H–C interactions at distances of 2.50 and 2.51 Å, with corresponding O...C separations of 3.11 and 3.14 Å. The formation of the three-dimensional hydrogen-bonded frameworks again resulted in the 4-fold interpenetration of the resulting architectures (Figure 13). The structure was not porous, with the NO₃[−] anions residing in small cavities between adjacent helices in a fashion similar to that in **4**. This resulted in the structure having no solvent accessible volume and a packing index of 0.75.³⁰

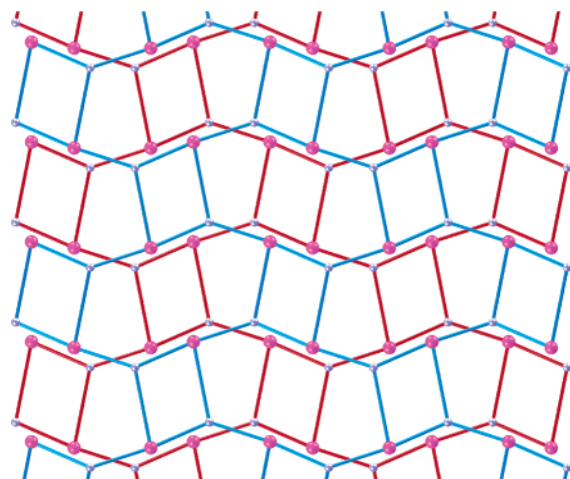


Figure 14. View of the topological networks of two adjacent sheets of **1** (Ag nodes, pink; N nodes, blue) showing the overlap of four-membered circuits with eight-membered circuits.

Topological Analyses. The topologies of complexes **1**, **3**, **4**, and **5** were determined using OLEX.³⁸ For topological analysis of supramolecular systems comprising one-dimensional coordination polymeric structures to be conducted, there must exist topologically significant interactions to link the individual polymer chains into a two- or three-dimensional net. For noncovalent interactions to be considered as forming a topologically significant network, they should be both strong and directional, such as hydrogen bonds^{1d,2,39} or electrostatic interactions occurring within van der Waals distances, but beyond previously recognized covalent bonding distances.⁴⁰ The absence of such topologically significant interactions between individual polymer chains in **2** meant that its topology was simply that of a zigzag chain.

For the topological analysis of **1**, the hydrogen bonds between CF₃SO₃[−] anions and amine N–H and the interactions between CF₃SO₃[−] anions and Ag^I cations were considered to be topologically significant. Because there were no interactions between two-dimensional sheets of the complex other than π -stacking, the topology was considered only for those sheets. The resulting topological network could be defined as a uninodal 4.8² net (Figure 14), with identical nodes based on Ag^I ions and the amine N of the **bpa** ligands. The ligand nodes had links to three metal nodes: two via the pyridine rings, one via the CF₃SO₃[−] anion. The metal nodes were also three-connected to ligand nodes, resulting in both nodes having short topological terms of 4.8². When the topological nets of adjacent sheets were examined, the four-membered circuits of one sheet were seen to overlies the eight-membered circuits of the next (Figure 14). The uninodal 4.8² net has been recognized as a two-dimensional network,⁴¹ and more recently, 4.8² connected nodes have

(38) Dolomanov, O. V.; Blake, A. J.; Champness, N. R.; Schröder, M. *OLEX; J. Appl. Crystallogr.* **2003**, *36*, 1283–1284.

(39) (a) Braga, D.; Maini, L.; Polito, M.; Grepioni, F. *Struct. Bonding* **2004**, *111*, 1–32. (b) Burrows, A. D. *Struct. Bonding* **2004**, *108*, 55–95.

(40) (a) Steed, J. W.; Atwood, J. L. *Supramolecular Chemistry*; John Wiley and Sons: Chichester, U.K., 2000; pp 19–30. (b) Lindoy, L. F.; Atkinson, I. M. *Self-Assembly in Supramolecular Systems*; Royal Society of Chemistry: Cambridge, U.K., 2000; pp 7–18.

been found to occur in a number of coordination polymeric⁴² and inorganic networks.⁴³ Two of the coordination polymeric systems and all of the inorganic systems displayed two-dimensional 4.8^2 sheets as part of a three-dimensional supramolecular array,^{42a,c,43} whereas the other two-dimensional coordination polymeric systems occur as both interpenetrated^{42d,e,i} and non-interpenetrated^{42a,b,f,g,h,j} two-dimensional structures. Two of the non-interpenetrated structures^{42h,j} were found to show the overlay of topological four-membered circuit on eight-membered circuit seen in this complex. In those structures, it was thought to prevent interpenetration of the frameworks.

For the topological analysis of **3**·**2MeCN**, the hydrogen bonds between ClO_4^- anions, MeCN solvent molecules, and amine N–H were considered to be topologically significant. Because there were no strong interactions between two-dimensional sheets of the complex, the topology could only be considered for those sheets. The topological network comprised two topologically identical nodes, based on the amine N atoms of the non-symmetry-related ligands. All nodes had the same short topological term, indicating that, topologically speaking, all nodes were the same. Each node had four links to adjacent nodes, one for each pyridine ring of the **bpa** ligands, and one for each pair of hydrogen-bonds linking the chains. All nodes had the short topological term of $4^4.6^2$, defining the framework as a (4, 4) net.⁴¹ Network structures with this topology are common among two-dimensional coordination polymers. Early examples of these structures were formed mostly using simple linear bridging ligands,⁴⁴ while more recent work has seen the use of more flexible and potentially complex ligands in the formation of these network architectures

Once again, for the topological analysis of **4**, the hydrogen-bonds between ClO_4^- anions and amine N–H were considered to be bonding interactions. Also, the electrostatic interactions between ClO_4^- anions and Ag^I cations, at 0.2 Å longer than reported bonding distances, were considered to be topologically significant. The resulting topological network was found to consist of 4-fold interpenetrated three-dimensional nets, in stark contrast to the two-dimensional

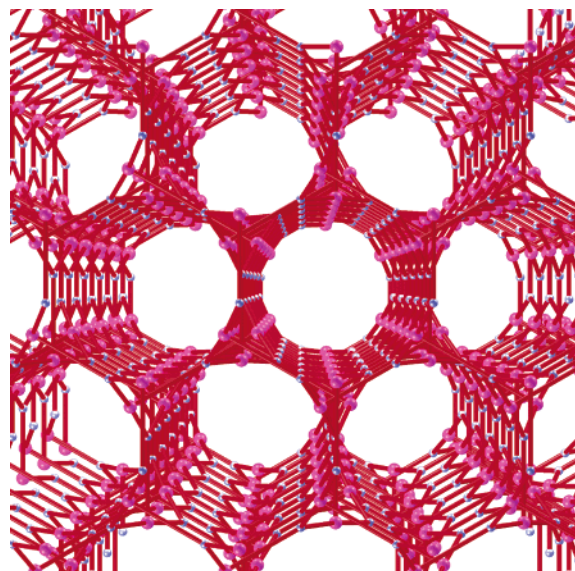


Figure 15. View of one (8, 3)-*a* topological net formed by **4**.

nets observed for **1** and **3**. The resulting topological networks could be defined as uninodal 8^3 nets, with identical nodes based on Ag^I ions and on the amine N atom of the **bpa** ligands (Figure 15). The ligand nodes had links to three metal nodes: two via the pyridine rings, and one via the ClO_4^- anion. The metal nodes were likewise three-connected to ligand nodes resulting in both nodes having short topological terms of 8^3 . The 8^3 net is one of the uniform nets discussed by Wells, and he defined 15 slightly different 8^3 nets as (8, 3)-*a* to -*o*.⁴¹ Based on his definitions, the structure of **4** would be an (8, 3)-*a* net. Despite the large number of possible different 8^3 nets, coordination polymeric materials containing them have been encountered only twice. The first structure, $\text{Na}[\text{Ti}_2(\text{PS}_4)_3]$,⁴⁵ formed an (8, 3)-*c* net, although the network type was not noted until its later study.⁴⁶ This structure was seen to display 2-fold interpenetration, in contrast to the 4-fold interpenetration shown by the three-dimensional net of **4**. A more recent study showed that the solvothermally crystallized complex $\{[\text{Cu}(\text{mtta})]\cdot 0.17\text{H}_2\text{O}\}_\infty$ (mtta = 5-methyltetrazolate) also formed an 8^3 net, although in this case, no interpenetration was observed.⁴⁷ Although the authors did not state which of Wells' networks they found their structure to be, analysis suggests it to be an (8, 3)-*b* net. Topologically, the only difference between these two nets is that the (8, 3)-*b* net displays both 3_1 and 3_2 helical elements, resulting in an achiral network, whereas the (8, 3)-*a* net only shows one enantiomer of the helix and as a result is chiral.⁴¹ The possibility that potential similarities in properties inherent to the network might exist between **4** and this Cu^I complex was considered. However, as one net is chiral and the other is not, and as the topological net of **4** was formed by weaker interactions as well as coordinate bonds and displayed 4-fold interpenetration, this seemed less likely.

- (41) Wells, A. F. *Three-Dimensional Nets and Polyhedra*; John Wiley and Sons: New York, 1977.
- (42) (a) Amoores, J. J. M.; Black, C. A.; Hanton, L. R.; Spicer, M. D. *Cryst. Growth Des.* **2005**, *5*, 1255–1261. (b) Fan, J.; Shu, M.-H.; Okamura, T.-a.; Li, Y.-Z.; Sun, W.-Y.; Tang, W.-X.; Ueyama, N. *New J. Chem.* **2003**, *27*, 1307–1309. (c) Fan, J.; Zhu, H.-F.; Okamura, T.-a.; Sun, W.-Y.; Tang, W.-X.; Ueyama, N. *New J. Chem.* **2003**, *27*, 1409–1411. (d) Fan, J.; Sun, W.-Y.; Okamura, T.-a.; Tang, W.-X.; Ueyama, N. *Inorg. Chem.* **2003**, *42*, 3168–3175. (e) Wan, S.-Y.; Fan, J.; Okamura, T.-a.; Zhu, H.-F.; Ouyang, X.-M.; Sun, W.-Y.; Ueyama, N. *Chem. Commun.* **2002**, 2520–2521. (f) Erxleben, A. *CrystEngComm* **2002**, *4*, 472–477. (g) Szklarzewicz, J.; Podgajny, R.; Lewiński, K.; Sieklucka, B. *CrystEngComm* **2002**, *4*, 199–201. (h) Long, D.-L.; Blake, A. J.; Champness, N. R.; Wilson, C.; Schröder, M. *Chem.—Eur. J.* **2002**, *8*, 2026–2033. (i) Barnett, S. A.; Blake, A. J.; Champness, N. R.; Nicolson, J. E. B.; Wilson, C. *J. Chem. Soc., Dalton Trans.* **2001**, 567–573. (j) Long, D.-L.; Blake, A. J.; Champness, N. R.; Schröder, M. *Chem. Commun.* **2000**, 1369–1370.
- (43) (a) Lin, Z.-E.; Zhang, J.; Zheng, S.-T.; Yang, G.-Y. *Z. Anorg. Allg. Chem.* **2005**, *631*, 155–159. (b) Gordon, L. E.; Harrison, W. T. A. *Acta Crystallogr., Sect. C* **2004**, *60*, m637–m639. (c) Ritchie, L. K.; Harrison, W. T. A. *Acta Crystallogr., Sect. C* **2004**, *60*, m634–m636.
- (44) Moulton, B.; Zaworotko, M. J. *Chem. Rev.* **2001**, *101*, 1629–1658 and references therein.

- (45) Cieren, X.; Angenault, J.; Couturier, J.-C.; Jaulmes, S.; Quarton, M.; Robert, F. *J. Solid State Chem.* **1996**, *121*, 230–235.
- (46) Batten, S. R.; Robson, R. *Angew. Chem., Int. Ed.* **1998**, *37*, 1460–1494.
- (47) Wu, T.; Yi, B.-H.; Li, D. *Inorg. Chem.* **2005**, *44*, 4130–4132.

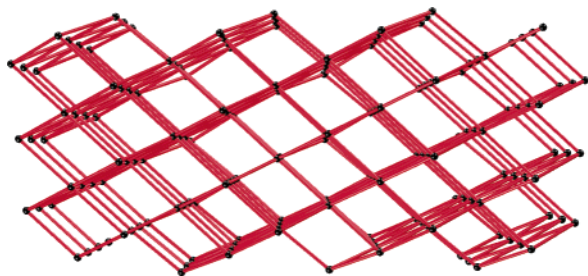


Figure 16. View of one of the α -polonium topological nets formed by **5** (NO_3^- nodes, black).

For the topological analysis of **5**, the hydrogen bonds between NO_3^- anions and the N–H of the amines were considered as being topologically significant. This again resulted in 4-fold interpenetrated three-dimensional nets in a manner akin to **4**, although the nets were seen to be significantly different. The resulting topological networks could be defined as uninodal $4^{12}.6^3$ nets, with nodes based on the N atom of the hydrogen-bonding NO_3^- anions. (Figure 16) Each node was linked to six other nodes via the polymer chains. The $4^{12}.6^3$ node topology is identical to that of the α -polonium network; however, in **5**, the networks display a skew not seen in the prototypical net. Despite the large number of octahedral transition-metal complexes, there are a lot fewer coordination polymers that display true six-connected nodes, although the number of such networks has been steadily increasing. The majority of these are related to the α -polonium net, with only six having an unrelated node topology.⁴⁸ Those related to the α -polonium net can be further divided into three major groups. The first contains those that adopt a true α -polonium type structure,⁴⁹ where all links between nodes are the same, and also includes skewed frameworks that result in rhombohedral cavities,⁵⁰ and the distorted α -polonium network, where there are two long links and four short between identical nodes.⁵¹ Among the α -polonium type structures also exists a subgroup of complexes based on metal–cyano salts, such as the Prussian-Blue-related networks.⁵² The second, and much smaller, group consists of those structures that adopt a network more

akin to the NaCl net, which is isotopological with the α -polonium net but consists of two equivalent octahedral nodes.⁵³ The third group is made up of those networks that may be simplified easily to α -polonium nets, but are more correctly described as nets with the boron topology of CaB_6 ,⁵⁴ which can be described as an α -polonium network with nodes replaced by octahedral clusters of nodes.⁴¹ These networks have been studied extensively by Yaghi and co-workers,⁵⁵ in particular the stability and gas sorption ability of the architectures. Other workers are now starting to design and construct similar network structures.⁵⁶ The frameworks formed by **1** were found to be most closely related to the rhombohedrally skewed α -polonium networks.

On first appearances, the modes of interpenetration shown by **4** and **5** do not appear to be the same as that seen for previously recognized architectures showing (8, 3) or α -polonium topologies, respectively. In the case of **4**, this difference in interpenetration mode is due to the network being an (8, 3)-*a* net, whereas the only previously reported complex showing an interpenetrating (8, 3) net was of the type (8, 3)-*c*,⁴⁵ which differs in structure because it is achiral. In **5**, the nets show a somewhat modified interpenetration mode. In the commonly seen mode of interpenetration in α -polonium nets, each cubic cavity interpenetrates eight others and vertexes of cubic cavities align on an internal diagonal,^{7f} whereas in a previously seen anomalous interpenetration mode, cubic cavities interpenetrated with 10 others.^{7f,57} The four interpenetrating nets in **5**, however, showed a mode different from either of these; each cubic cavity interpenetrated with eight others, but the four independent nets did not align vertexes along an internal diagonal.

Conclusion

Five different complexes of Ag^I salts and **bpa** were prepared and characterized. All the complexes showed a linear coordination geometry of **bpa** about the Ag^I ions, with in one case an additional molecule of MeCN solvent coordinated. This linear geometry led to the formation of three zigzag and two helical complexes, all of which were held together by extensive intermolecular interactions. Both

(48) (a) Williams, C. A.; Blake, A. J.; Hubberstey, P.; Schröder, M. *Chem. Commun.* **2005**, 5435–5437. (b) Rizk, A. T.; Kilner, C. A.; Halcrow, M. A. *CrystEngComm* **2005**, *7*, 359–362. (c) Zhao, X.-J.; Batten, S. R.; Du, M. *Acta Crystallogr., Sect. E* **2004**, *60*, m1237–m1239. (d) Li, J.-R.; Zhang, R.-H.; Bu, X.-H. *Cryst. Growth Des.* **2004**, *4*, 219–221. (e) Su, C.-Y.; Cai, Y.-P.; Chen, C.-L.; Kang, B.-S. *Inorg. Chem.* **2001**, *40*, 2210–2211. (f) Lin, W.; Wang, Z.; Ma, L. *J. Am. Chem. Soc.* **1999**, *121*, 11249–11250.

(49) For example, see: (a) Long, D.-L.; Hill, R. J.; Blake, A. J.; Champness, N. R.; Hubberstey, P.; Wilson, C.; Schröder, M. *Chem.–Eur. J.* **2005**, *11*, 1384–1391. (b) Goodgame, D. M. L.; Grachvogel, D. A.; Hussain, I.; White, A. J. P.; Williams, D. J. *Inorg. Chem.* **1999**, *38*, 2057–2063. (c) Duncan, P. C. M.; Goodgame, D. M. L.; Menzer, S.; Williams, D. J. *Chem. Commun.* **1996**, 2127–2128. (d) Brodtkin, J. S.; Foxman, B. M. *J. Chem. Soc., Chem. Commun.* **1991**, 1073–1075.

(50) For example, see: (a) Chen, X.-Y.; Zhao, B.; Shi, W.; Xia, J.; Cheng, P.; Liao, D.-Z.; Yan, S.-P.; Jiang, Z.-H. *Chem. Mater.* **2005**, *17*, 2866–2874. (b) Abrahams, B. F.; Hoskins, B. F.; Robson, R.; Slizys, D. A. *CrystEngComm* **2002**, *4*, 478–482.

(51) For example, see: (a) Chen, B.; Fronczek, F. R.; Courtney, B. H.; Zapata, F. *Cryst. Growth Des.* **2006**, *6*, 825–828. (b) Noro, S.-i.; Kitagawa, S.; Kondo, M.; Seki, K. *Angew. Chem., Int. Ed.* **2000**, *39*, 2081–2084. (c) Subramanian, S.; Zaworotko, M. J. *Angew. Chem., Int. Ed.* **1995**, *34*, 2127–2129. (d) Soma, T.; Yuge, H.; Iwamoto, T. *Angew. Chem., Int. Ed.* **1994**, *33*, 1665–1666.

(52) For example, see: (a) Liu, C.-M.; Gao, S.; Kou, H.-Z.; Zhang, D.-Q.; Sun, H.-L.; Zhu, D.-B. *Cryst. Growth Des.* **2006**, *6*, 94–98. (b) Goodwin, A. L.; Chapman, K. W.; Kepert, C. J. *J. Am. Chem. Soc.* **2005**, *127*, 17980–17981. (c) Hoskins, B. F.; Robson, R.; Scarlett, N. V. *J. Chem. Soc., Chem. Commun.* **1994**, 2025–2026.

(53) Goodgame, D. M. L.; Grachvogel, D. A.; White, A. J. P.; Williams, D. J. *Inorg. Chim. Acta* **2003**, *344*, 214–220. (b) Hoskins, B. F.; Robson, R.; Slizys, D. A. *Angew. Chem., Int. Ed.* **1997**, *36*, 2752–2755.

(54) O’Keeffe, M.; Hyde, B. G. *Crystal Structures I: Patterns and Symmetry*; Mineralogy Society of America: Washington, DC, 1996.

(55) For example, see: (a) Rosi, N. L.; Kim, J.; Eddaoudi, M.; Chen, B.; O’Keeffe, M.; Yaghi, O. M. *J. Am. Chem. Soc.* **2005**, *127*, 1504–1518. (b) Rowsell, J. L. C.; Millward, A. R.; Park, K. S.; Yaghi, O. M. *J. Am. Chem. Soc.* **2004**, *126*, 5666–5667. (c) Eddaoudi, M.; Kim, J.; Rosi, N. L.; Vodak, D.; Wachter, J.; O’Keeffe, M.; Yaghi, O. M. *Science* **2002**, *295*, 469–472. (d) Kim, J.; Chen, B.; Reinke, T. M.; Li, H.; Eddaoudi, M.; Moler, D. B.; O’Keeffe, M.; Yaghi, O. M. *J. Am. Chem. Soc.* **2001**, *123*, 8239–8247.

(56) Zhang, J.-J.; Sheng, T.-J.; Hu, S.-M.; Xia, S.-Q.; Leibling, G.; Meyer, F.; Fu, Z.-Y.; Chen, L.; Fu, R.-B.; Wu, X.-T. *Chem.–Eur. J.* **2004**, *10*, 3963–3969.

(57) Hong, C. S.; Son, S. K.; Lee, Y. S.; Jun, M.-J.; Do, Y. *Inorg. Chem.* **1999**, *38*, 5602–5610.

of the helical complexes were also found to form interpenetrating three-dimensional networks. Surprisingly, it was noted that the zigzag complexes, which had as anions CF_3SO_3^- (**1**), PF_6^- (**2**·MeCN), and ClO_4^- (**3**·2MeCN), all had incorporated MeCN solvent molecules, whereas both of the helical complexes, with ClO_4^- (**4**) and NO_3^- (**5**), showed efficient packing without the need to incorporate any solvent. None of these five complexes showed coordination of the anion, although the helical ClO_4^- complex (**4**) showed an interaction between the Ag^+ cation and the anion. In all other cases, the anions, along with noncoordinated solvent, were held in place in the structures by hydrogen bonding supported by other weak interactions.

The most important of the additional supramolecular functionalities in **bpa** was found to be the amine group acting as a hydrogen-bonding synthon. The hydrogen bonds usually increased the dimensionality of the networks being formed. Slightly less important were the aromatic rings of **bpa**. These rings permitted the formation of a number of different π -interactions in the complexes. The previously unexplored axial helicity of **bpa** in the solid state was also shown to be a factor in the formation of complexes. In these one-dimensional polymeric structures, its ability to behave as a two-bladed chiral molecular propeller has led to the synthesis of conglomerates consisting of both enantiomerically pure and racemically twinned helical coordination polymers, as well as achiral systems.

The supramolecular interactions between polymer chains led to the formation of two- or three-dimensional architectures, and for **4** and **5**, gave rise to interpenetrated nets. In all complexes except that of **2**, the topology of the two- or three-dimensional nets were studied. The two two-dimensional nets formed by **1** and **3** were different because of the different hydrogen-bonding modes. The topological nets formed by **4** and **5** were both found to be three-dimensional. Only one topological net was possible for **4**, which was Wells' uncommon chiral (8, 3)-*a* net, whereas the networks formed in **5** showed the α -polonium network topology.⁴¹

Over the five complexes, it appeared that the use of different anions had subtle effects on the resulting coordina-

tion polymers. As none of them coordinated to the Ag^+ ions, they did not affect the structure by varying coordination. Despite the volume and shape differences of the anions involved, they interacted in similar ways with the cationic framework, by either forming noncoordinate interactions to Ag^+ or hydrogen bonding to the amine N–H. They also all formed a number of weak interactions with either the pyridine rings of the **bpa** ligands or the solvent molecules. In complex **5**, the NO_3^- anions interacted in a highly symmetric fashion with the cationic framework. These interactions took place as bifurcated hydrogen bonds, with two NO_3^- O atoms interacting with the amine N–H of three surrounding polymeric chains. As the anions were not coordinated, they were available to play a true templating role in the formation of the three-dimensional networks.⁸ The symmetry and strength of the interactions between NO_3^- anions and helices suggested the anions played an important role in templating the three-dimensional hydrogen-bonded network of helices that formed. Further support of this was seen in the ability to prepare this network structure using both traditional methods of crystallization and hydrothermal synthesis, in contrast to the different structures observed for complexes **3**·2MeCN and **4**.

This work shows the subtle effect on coordination polymers of counterion and solvent when associated with a well-defined hydrogen-bonding synthon. Many of these subtleties could not have been appreciated without detailed topological analysis.

Acknowledgment. We thank Professor Ward T. Robinson and Dr. Jan Wikaira (University of Canterbury) for X-ray data collection and the University of Otago Research Committee and the Department of Chemistry, University of Otago, for financial support.

Supporting Information Available: An X-ray crystallographic file in CIF format for the structure determination of **bpa** and **1–5**, full topological analyses for complexes **1**, **3**·2MeCN, **4**, and **5**. This material is available free of charge via the Internet at <http://pubs.acs.org>.

IC060487Y